ARTICLES

Journal of Semiconductors
(2019) 40, 062004
doi: 10.1088/1674-4926/40/6/062004

Electronic band structures and optical properties of atomically thin AuSe: first-principle calculations

Pengxiang Bai, Shiying Guo, Shengli Zhang†, Hengze Qu, Wenhan Zhou, and Haibo Zeng†

MIIT Key Laboratory of Advanced Display Materials and Devices, School of Materials Science and Engineering, Nanjing University of Science and Technology, Nanjing 210094, China

Abstract: As a large family of 2D materials, transition metal dichalcogenides (TMDs) have stimulated numerous works owing to their attractive properties. The replacement of constituent elements could promote the discovery and fabrication of new nanofilm in this family. Using precious metals, such as platinum and palladium, to serve as transition metals combined with chalcogen is a new approach to explore novel TMDs. Also, the proportion between transition metal and chalcogen atoms is found not only to exist in conventional form of 1 : 2. Herein, we reported a comprehensive study of a new 2D precious metal selenide, namely AuSe monolayer. Based on density functional theory, our result indicated that AuSe monolayer is a semiconductor with indirect band-gap of 2.0 eV, which possesses superior dynamic stability and thermodynamic stability with cohesive energy up to –7.87 eV/atom. Moreover, it has been confirmed that ionic bonding predominates in Au–Se bonds and absorption peaks in all directions distribute in the deep ultraviolet region. In addition, both vibration modes dominating marked Raman peaks are parallel to the 2D plane.

Key words: AuSe monolayer; DFT calculation; 2D semiconductor

Citation: P X Bai, S Y Guo, S L Zhang, H Z Qu, W H Zhou, and H B Zeng, Electronic band structures and optical properties of atomically thin AuSe: first-principle calculations[J]. *J. Semicond.*, 2019, 40(6), 062004. http://doi.org/10.1088/1674-4926/40/6/062004

1. Introduction

Tracing back to the process of human exploring two-dimension (2D) material, there is no doubt that the discovery of graphene is the originator[1]. In the following decade, a great number of layered materials have been focused on and exfoliated to nano-sheet, in order to replace zero band-gap graphene and be applied to thin-film transistor (TFT). Transition metal dichalcogenides (TMDs), represented by MoS_2, consecutively inspired researches to study them as a family[2–5]. Even though MoS_2 possesses suitable band-gap for semiconducting application, low mobility of 200–500 $cm^2 V^{-1}s^{-1}$ largely limits its application potential in high speed devices. In a few short years, chalcogen of TMDs has been extended to group VI elements like selenium and tellurium, while metallic elements also have been covered numerous transition metals[6–8].

Over past several years, precious metal related TMDs also came into the view of researches and some attractive properties were founded among them. For instance, on the one hand, PtS_2 and $PtSe_2$ have strongly bound excitons and rather high mobility[9–12], on the other hand, $PbSe_2$ has considerable Seebeck coefficient and on/off ratio[13], and PbS_2 holds unique structural characteristics[14]. Meanwhile, multiple stoichiometric ratio between transition metals and chalcogen beyond traditional form were also revealed, like Au_6S_2 with direct band-gap and distinguished mobility of 2721 $cm^2 V^{-1} s^{-1}$[15], Ag_2S with unique bi-directional auxetic property[16]. A lot of novel properties, other than those of common TMDs reported before, were revealed among them. Gold–selenide (AuSe), as a layered material with Van der Waal's interaction between adjacent layers of bulk phase, has also been synthesised to 2D form[17]. Even though, less work was done for further property study.

In this article, all theoretical studies on AuSe monolayer were performed within first-principle calculations. Optimized structure is composed by tri-coordinated Se atoms, tetra- and two-coordinated Au atoms, Se atoms of which grant it zigzag appearance. Double stability (dynamic and thermodynamic stability) was demonstrated by phonon dispersion and cohesive energy calculations. Our calculation results of electronic structure and optical properties revealed that AuSe monolayer is a semiconductor with an indirect band-gap of 2.0 eV, and sensitively responds to deep-UV light. All of computation and discussion done in this reported are significative to better exhibit this precious metal related transition metal selenide.

2. Computational methods

All first-principle calculations were performed on the bias of density functional theory (DFT) as implement in CASTEP code[18] except VASP code[19] only for electron localization function (ELF), cleavage energy and electronic density of the highest occupied band (VBM) and the lowest unoccupied band (CBM). Perdew-Burke-Ernzerh (PBE) of generalized gradient approximation (GGA) functional were employed for exchange-correlation interaction[20]. The cut-off energy of plane-wave basis for all calculations was set as 610 eV. Optimization of geometric structure was relaxed until the total energy and maximum residual force are lower than 5×10^{-6} eV/atom and

Correspondence to: S L Zhang, zhangslvip@njust.edu.cn; H B Zeng, zeng.haibo@njust.edu.cn

Received 26 MARCH 2019; Revised 5 MAY 2019.

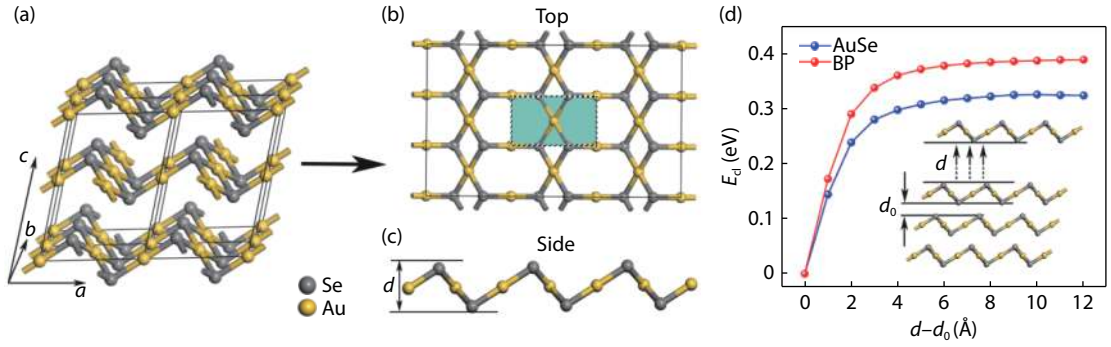

Fig. 1. (Color online) Structure of (a) bulk AuSe with 2 × 2 × 1 supercell, (b) two dimensional AuSe in top view and (c) side view. (d) Cleavage energy of AuSe monolayer and black phorphous.

Table 1. Optimized lattice parameters of AuSe monolayer.

Material	Bond length (Å)		Bond angle (deg)			Lattice parameters (deg)	
	d_1	d_2	θ_1	θ_2	θ_3	α	γ
AuSe	2.49	2.41	94.73	85.27	97.45	90.00	84.13

0.01 eV/Å, respectively. Sufficient thickness of 20 Å was initially set for vacuum space along *c*-axis to fully eliminate the interaction between layers. Since that band-gap trends to be underestimated by using PBE functional, the calculation of band structure was also performed based on the hybrid functional of Heyd-Scuseria-Ernzerh (HSE06)[21, 22]. Sample mode in the first Brillouin zone was set as 4 × 2 × 1 Monkhorst–Pack *k*-grid.

3. Result and discussion

3.1. Geometric optimized structure of AuSe monolayer

All geometric structural models of bulk and monolayer AuSe are shown in Fig. 1. One could see a clear layered structure in bulk AuSe, indicating 2D AuSe could be easily fabricated by overcoming its weak Van der Waals' coupling between layers. Atomically thin AuSe exhibits unique hexagon-rhombus combined configuration from the top view, and similar buckled structure with group-V 2D materials (phosphorene, arsenene and antimonene) from the side view[23–28]. The crystal symmetry of AuSe monolayer is decided by space group P2/m, and the unit cell is marked by coloured region. For the specific information of structure, optimized lattice constants $a = 6.40$ Å and $b = 3.67$ Å, respectively, and then the thickness (d) of single layer sheet is 2.50 Å. Sp^3-hybridized selenium atoms, which endow AuSe monolayer a buckled layer, coordinate with three gold atoms, while there are two different coordination forms, tetra-coordination and two-coordination, for gold atoms. Other detailed parameters including bond length and angle are summarized in Table 1. The feasibility of peeling layered materials from their bulk counterparts can be effectively judged by cleavage energies comparison. Those bulk ones with lower cleavage energies are promising to be lightly fabricated to 2D forms by common mechanical exfoliation or liquid exfoliation. In view of this, cleavage energy calculation is performed and the result is shown in Fig. 1(c), where energy increases with the interlayer distance and converges to 0.32 J/m^2. As a comparison, cleavage energy changing curve of black phosphorus is also presented, whose converged energy is even higher than AuSe. Therefore, to synthesize AuSe monolayer by mechanically peeling is more likely to be realized.

3.2. Stability and Raman scattering

Stability is crucial to applying 2D materials to electronic devices. Dynamic stability of crystals can be directly confirmed by calculating the dispersion of phonon band. Hence, the phonon spectrum is simulated and presented in Fig. 2(a) for studying the dynamical stability of AuSe monolayer. All frequencies of lattice vibration are positive, namely, no imaginary modes occur in the entire Brillouin path, indicating AuSe monolayer possesses superior kinetic stability. Cohesive energy is another factor for stability which is often used to judge robust bonding. The specific value is defined as:

$$E_{\mathrm{coh}} = -\frac{nE_{\mathrm{Au}} + nE_{\mathrm{Se}} - E_{\mathrm{AuSe}}}{2n}, \quad (1)$$

where E_{Au}, E_{Se} and E_{AuSe} represent the energy of single gold atom, single selenium atom and AuSe monolayer, respectively, and n denotes the numbers of gold or selenium atoms in AuSe monolayer. The computation result is up to –7.87 eV/atom, which is comparable to that of graphene and h-BN[29–31]. From another point of view, utilizing the energies of bulk Au and Se crystals as a reference is necessary. It is reasonable to calculate the energy change, from bulk Au and Se crystals to 2D AuSe phase during phase transition, as a powerful evidence of stable 2D AuSe crystal. Utilizing the same formula and substituting single atom energy with bulk crystal energy, the cohesive energy is –0.29 eV/atom, which presents prospective negative value. In these two regards, the extraordinary thermodynamic stability of AuSe monolayer is also expected.

In order to reveal information about molecules vibration and rotation in AuSe monolayer, we simulated the Raman scattering spectrum. As shown in Fig. 2(b), there are two remarkable Raman peaks appearing at 168.8 and 203.3 nm, which stem from vibration modes of B_g and A_g, respectively. The intensity of the B_g peak is much stronger than that of A_g, indicating the B_g mode predominates over the A_g mode. In addition, both two modes are corresponding to the frequency of phonons at the centre of Brillouin zone (Gamma point), which could be traced from phonon spectrum. More visualized sketches of vibration modes are inserted in the spectrum beside corres-

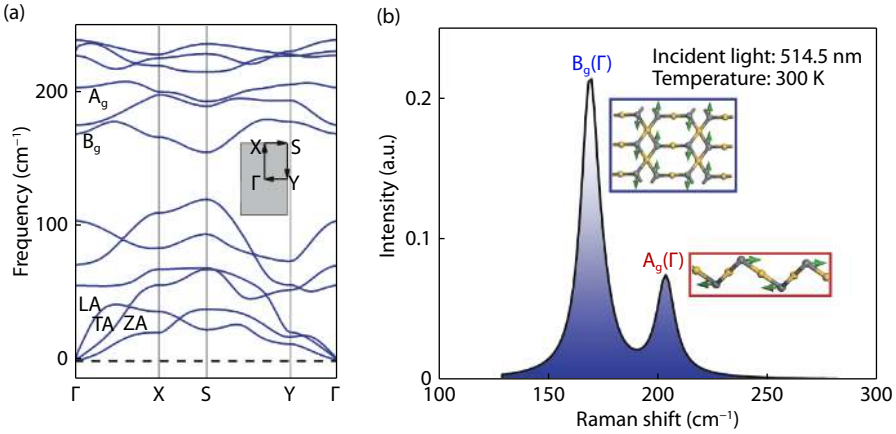

Fig. 2. (Color online) (a) Phonon spectrum of AuSe monolayer. (b) Simulation spectrum of Raman shift with exciting wavelength of 514.5 nm at 300 K and corresponding schematic diagram of vibration modes (inset).

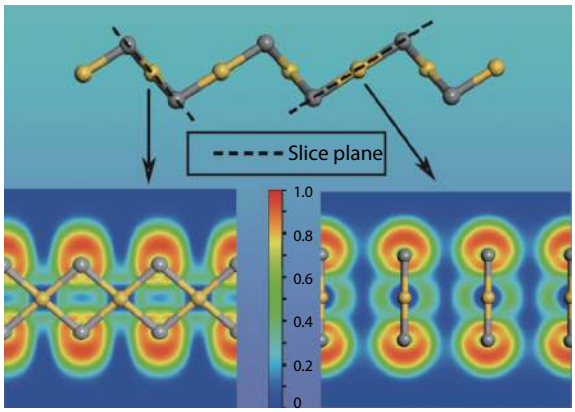

Fig. 3. (Color online) Electron localization function (ELF) maps of AuSe monolayer, where blue and red regions denote accumulation and depletion of electrons, respectively.

ponding peaks, showing that both of them vibrate within the layered plane while no vibration modes is perpendicular to the plane.

3.3. Chemical bonding

Two different coordination forms of gold atoms in AuSe monolayer attract our interest to reveal the types of chemical bonding in this ultrathin crystal. Electron localization function (ELF) is usually computed to obtain the localization of electrons around atoms or along chemical bonds and further to judge the types of chemical bonding[32]. The large value of 1.0 signifies strongly localized electrons, and the small value closed to 0 refers to the depletion of electrons. Moreover, median of 0.5 represents highly delocalized of electrons. Fig. 3 shows ELF maps in two characteristic slice planes of AuSe monolayer. Aspherically symmetric localized electrons mainly distribute around Se atoms accompanied with low charge density appears around Au atoms, indicating ionic bonding is predominant. Strong localization of electrons distribute on the top and bottom of 2D plane, deriving from symbolic lone pairs on the surface of nano-materials. One should be noted that relatively obvious delocalized electrons are located around outer shell of Au sites, implying some valence electrons sharing feature of covalent bonding, though it is very weak.

3.4. Electronic structure

The electronic properties are vital for applying new 2D materials to atomically thin nano-electronic components and transistors. The band structure calculated by using HSE06 and GGA-PBE functional are shown in Fig. 4(a), together with density of states (PBE) near fermi level. The bandstructure calculated at all functional levels indicates AuSe monolayer is an indirect band gap semiconductor. The band gap calculated at PBE level is widely known underestimated in recent years, therefore a more precise result of 2.0 eV is obtained by HSE06 functional. Spin orbit coupling (SOC) has been reported to strongly affect bandsturcture of heavier elements related compounds, basing bandstructure inversion mechanism in topological insulators, which is crucial to explain the occurrence of edge states. For more complete characteristic revelation of this emerging material, bandstructure with SOC effect is also calculated at PBE level. However, the result in Fig. 4(a) shows no evident difference after considering SOC effects, only presenting some gap shrink. Hence, AuSe monolayer is a new 2D semiconductor with a medium band-gap. Moreover, the variation trend of valence band maximum is quite different along various *k*-path, implying different hole effective mass along them, which is calculated by:

$$m_{\mathrm{p}}^{*} = -\hbar^{2}\left(\frac{\partial^{2}E}{\partial k^{2}}\right)^{-1}, \tag{2}$$

where $\hbar$ is the reduced Plank constant, k and E represent the wave vector and corresponding energy, respectively. For the energy variation along Y–S direction is more smooth than Y–Γ direction, the effective mass of holes along *a* direction in AuSe monolayer is lighter than that of *b* direction. Hence, one could be inferred that prominent anisotropic hole mobility probably exists.

According to the density of states around fermi level, both valence band maximum (VBM) and conduction band minimum (CBM) are mainly dominated by p-orbit while d-orbital contribution is minor. To further obtain specific contribution at atomic resolution, charge density for CBM and VBM are shown in Figs. 4(b) and 4(c), respectively. The domination of p-orbit belongs to Se and d-orbit only derives from Au. Something interesting is that there is little electronic states contribution of CBM for the gold atoms in the centre of unit cell. And the reason behind this is that all valence electrons of 4-coordination gold atoms are assigned to bonding state, lacking the states of anti-bonding.

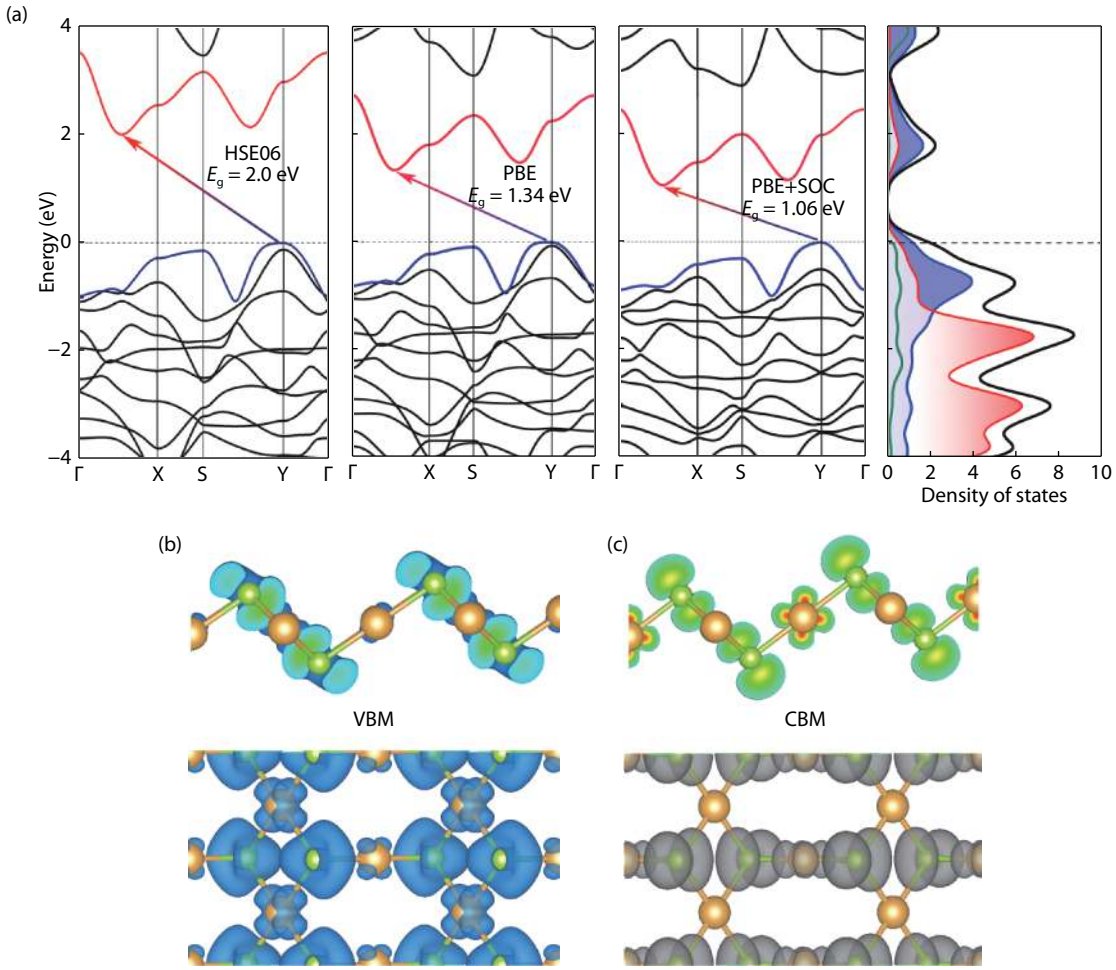

Fig. 4. (Color online) (a) Computed band structure and density of states (DOS) of AuSe monolayer at HSE06, PBE and PBE+SOC levels, charge density of (b) VBM and (c) CBM, isosurface level is 0.0052 e/bohr^3.

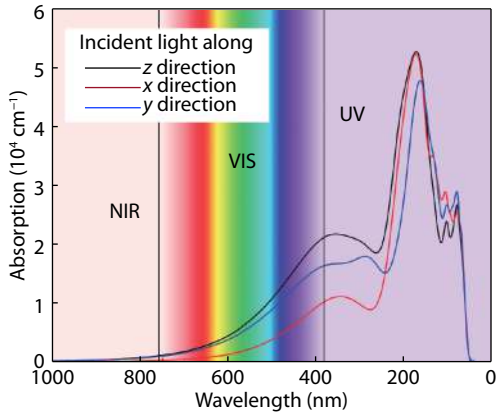

Fig. 5. (Color online) Absorption spectrum of AuSe monolayer with incident light perpendicular to the 2D plane (*z* direction) and along different directions in the plane (*x* and *y* directions).

3.5. Optic properties

Optical absorption properties are also carried out by calculating absorption coefficient from ultraviolet-visible (UV–VIS) to near-infrared (NIR) band with HSE06 functional. Since the majority of 2D materials exhibit anisotropic optical properties, the simulative incident light (unpolarized) is set along different directions in and out of plane. The result is shown in Fig. 5. Sharp absorption peaks of all cases occur along deep-UV region, which indicates the optical band-gap of AuSe monolayer is much larger than the electronic band-gap. It results from that the participation of phonon will consume a large quantity of energy during electrons jumping in indirect band-gap semiconductors. The absorption coefficient along *y* direction is obviously higher than *x* direction in NIR–VIS band and occurs blue-shift in UV band, confirming its anisotropy as expected before. Meanwhile, the coefficient along *z* direction is higher than both *x* and *y* directions in *xy* plane. The sensitive response to the deep-UV light is below 200 nm in all directions, underlying the future application in C-type deep-UV (below 240 nm) optoelectronic device like some III-borides including AlN and BN[33, 34]. It is also significant in exploitation fields of solar-blind photoelectric detection, environmental monitoring, and even ultraviolet communication. These tempting prospects derive from the scarcity of deep-UV light near the Earth's surface, thereby avoiding the interference of ambient light in a large extent.

4. Conclusion

In conclusion, by simulation and calculation with DFT, we predicted a new precious metal related material monolayer gold-selenide, namely 2D AuSe. Optimized structure, cleavage energy, phonon and Raman scattering, electronic distribute and structural properties, absorption coefficient were calculated to study a series of properties it possesses. As a result, we

concluded it is an indirect band-gap semiconductor with superb dynamic and thermodynamic stability. Especially for thermodynamics, cohesive energy of AuSe monolayer is up to -7.87 eV/atom. Ionic bonds are predominant between selenium and gold atoms. All feature peaks of Ranman spectrum correspond to in-plane vibration, and the sensitive response band in AuSe monolayer is located in deep-UV region with absorption peaks occur around 200 nm. All works we have discussed in this report would have meaningful value for deeper research and applications of AuSe monolayer.

Acknowledgements

This work was financially supported by the Natural Science Foundation of Jiangsu Province (No. BK20180071), the Fundamental Research Funds for the Central Universities (No. 30919011109) and PAPD of Jiangsu Higher Education Institutions.

References

[1] Novoselov K S, Geim A K, Morozov S V, et al. Electric field effect in atomically thin carbon films. Science, 2004, 306, 666
[2] Mak K F, Lee C, Hone J, et al. Atomically thin MoS_2: a new direct-gap semiconductor. Phys Rev Lett, 2010, 105, 136805
[3] Radisavljevic B, Radenovic A, Brivio J, et al. Single-layer MoS_2 transistors. Nat Nanotechnol, 2011, 6, 147
[4] Wang Q H, Kalantar-Zadeh K, Kis A, et al. Electronics and optoelectronics of two-dimensional transition metal dichalcogenides. Nat Nanotechnol, 2012, 7, 699
[5] Zhang Y, Ye J, Matsuhashi Y, et al. Ambipolar MoS_2 thin flake transistors. Nano Lett, 2012, 12, 1136
[6] Mak K F, Shan J. Photonics and optoelectronics of 2D semiconductor transition metal dichalcogenides. Nat Photon, 2016, 10, 216
[7] Tan C, Zhang H. Two-dimensional transition metal dichalcogenide nanosheet-based composites. Chem Soc Rev, 2015, 44, 2713
[8] Yun W S, Han S W, Hong S C, et al. Thickness and strain effects on electronic structures of transition metal dichalcogenides: 2H-MX_2 semiconductors (M = Mo, W; X = S, Se, Te). Phys Rev B, 2012, 85, 033305
[9] Sajjad M, Singh N, Schwingenschlögl U. Strongly bound excitons in monolayer PtS_2 and $PtSe_2$. Appl Phys Lett, 2018, 112, 043101
[10] Wang Y, Li L, Yao W, et al. Monolayer $PtSe_2$, a new semiconducting transition-metal-dichalcogenide, epitaxially grown by direct selenization of Pt. Nano Lett, 2015, 15, 4013
[11] Yim C, Lee K, McEvoy N, et al. High-performance hybrid electronic devices from layered $PtSe_2$ films grown at low temperature. ACS Nano, 2016, 10, 9550
[12] Zhang K, Yan M, Zhang H, et al. Experimental evidence for type-II Dirac semimetal in $PtSe_2$. Phys Rev B, 2017, 96, 125102
[13] Sun J F, Shi H L, Siegrist T, et al. Electronic, transport, and optical properties of bulk and mono-layer $PdSe_2$. Appl Phys Lett, 2015, 107, 153902
[14] Wang Y, Li Y, Chen Z. Not your familiar two dimensional transition metal disulfide: structural and electronic properties of the PdS_2 monolayer. J Mater Chem C, 2015, 3, 9603
[15] Wu Q, Xu W W, Qu B, et al. Au_6S_2 monolayer sheets: metallic and semiconducting polymorphs. Mater Horiz, 2017, 4, 1085
[16] Peng R, Ma Y, He Z, et al. Single-layer Ag_2S: A two-dimensional bidirectional auxetic semiconductor. Nano Lett, 2019, 19(2), 1227
[17] Machogo L F E, Tetyana P, Sithole R, et al. Unravelling the structural properties of mixed-valence α- and β-AuSe nanostructures using XRD, TEM and XPS. Appl Surf Sci, 2018, 456, 973
[18] Clark S J, Segall M D, Pickard C J, et al. First principles methods using CASTEP. Z Kristallogr, 2005, 220, 567
[19] Kresse G, Furthümller J. Efficient iterative schemes for ab initio total-energy calculations using a plane-wave basis set. Phys Rev B, 1996, 54, 11169
[20] Perdew J P, Burke K, Ernzerhof M. Generalized gradient approximation made simple. Phys Rev Lett, 1996, 77, 3865
[21] Heyd J, Scuseria G E, Ernzerhof M. Hybrid functionals based on a screened Coulomb potential. J Chem Phys, 2003, 118, 8207
[22] Paier J, Marsman M, Hummer K, et al. Screened hybrid density functionals applied to solids. J Chem Phys, 2006, 124, 154709
[23] Liu H, Neal A T, Zhu Z, et al. Phosphorene: An unexplored 2D semiconductor with a high hole mobility. ACS Nano, 2014, 8, 4033
[24] Li L, Yu Y, Ye G J, et al. Black phosphorus field-effect transistors. Nat Nanotechnol, 2014, 9, 372
[25] Qiao J, Kong X, Hu Z X, et al. High-mobility transport anisotropy and linear dichroism in few-layer black phosphorus. Nat Commun, 2014, 5, 4475
[26] Zhang S, Guo S, Chen Z, et al. Recent progress in 2D group-VA semiconductors: from theory to experiment. Chem Soc Rev, 2018, 47, 982
[27] Zhang S, Xie M, Li F, et al. Semiconducting group 15 monolayers: a broad range of band gaps and high carrier mobilities. Angew Chem Int Ed Engl, 2016, 55, 1666
[28] Zhang S, Yan Z, Li Y, et al. Atomically thin arsenene and antimonene: semimetal–semiconductor and indirect-direct band-gap transitions. Angew Chem Int Ed Engl, 2015, 54, 3112
[29] Koskinen P, Malola S, Hakkinen H. Self-passivating edge reconstructions of graphene. Phys Rev Lett, 2008, 101, 115502
[30] Şahin H, Cahangirov S, Topsakal M, et al. Monolayer honeycomb structures of group-IV elements and III–V binary compounds: First-principles calculations. Phys Rev B, 2009, 80, 155453
[31] Topsakal M, Aktürk E, Ciraci S. First-principles study of two- and one-dimensional honeycomb structures of boron nitride. Phys Rev B, 2009, 79, 115442
[32] Silvi B, Savin A. Classification of chemical bonds based on topological analysis of electron localization functions. Nature, 1994, 317, 683
[33] Li J, Fan Z Y, Dahal R, et al. 200 nm deep ultraviolet photodetectors based on AlN. Appl Phys Lett, 2006, 89, 213510
[34] Sajjad M, Jadwisienczak W M, Feng P. Nanoscale structure study of boron nitride nanosheets and development of a deep-UV photo-detector. Nanoscale, 2014, 6, 4577